Supplementary Material for DT-COM-06-2015-002457

Unexpected Synthesis of an Au_2In_2 Tetrametallatricyclic Complex from α-Aminophosphines and Formation of Au-In-P and Ag-In-P Nanomaterials

Hsiao Wei Chen,[a] T. S. Andy Hor,*[a, b] Roberto Pattacini,[c] and Pierre Braunstein*[c]

Experimental Section

General Procedures and Materials

All reactions were performed under purified nitrogen atmosphere using standard Schlenk techniques and distilled solvents. Recrystallizations of the products were performed in air. [AuCl(THT)][1] and **1a**[2] were prepared according to literature procedures. All other reagents used were AR quality obtained from commercial sources and used as received.

Nuclear Magnetic Resonance (NMR) Spectroscopy

All ^{1}H NMR (δ (TMS) = 0.0 ppm), $^{13}C\{^{1}H\}$ NMR (δ(TMS) = 0.0 ppm) and $^{31}P\{^{1}H\}$ NMR (δ(85% H_3PO_4) = 0.0 ppm) spectra were recorded at *ca.* 300 K at operating frequencies of 500.13, 125.73 and 202.45 MHz, respectively, on a Bruker AMX 500 MHz instrument. All $^{19}F\{^{1}H\}$ NMR (δ(TFA) = 0.0 ppm) were recorded at *ca.* 300 K at operating frequencies of 282.28 MHz on a Bruker ACF 300 MHz instrument.

Elemental Analyses

Elemental analyses were performed by the Chemical, Molecular and Materials Analysis Center (CMMAC) NUS, on a Perkin Elmer PE 2400 CHNS analyser.

ESI-MS

ESI-MS were obtained with a Finnigan/MAT LCQ mass spectrometer coupled with a TSP4000 HPLC system and the crystal 310 CE systems. Peaks were assigned from the *m/z* values.

Single Crystal X-ray Diffraction

Single crystal X-ray diffraction data were collected on a Bruker AXS CCD diffractometer using the Mo-Kα radiation (λ= 0.71073 Å). The software SMART[3] was used for data frame collection, indexing reflections, and determining lattice parameters. Integration of the reflections intensity and scaling were done by using SAINT[3] and SADABS[4] was used for empirical absorption correction and SHELXTL[5] for space group determination, refinements, graphics and structure reporting. The structures were solved by direct methods to locate the heavy atoms, followed by difference maps for the light non-hydrogen atoms. Anisotropic thermal parameters were defined for the rest of the non-hydrogen atoms. The hydrogen atoms were placed in their ideal positions when possible. The data collection parameters of complex **2**·$(OTf)_2$·$4H_2O$ and **3b** are listed in Table S1.

The structure of **2**·$(OTf)_2$·$4H_2O$ was further refined with disordered treatments of tetrahydrothiophene oxide and two OTf counterions. The asymmetric contains two disordered OTf anions. The hydrogen atoms on the coordinated H_2O were located from difference Fourier map while those on the uncoordinated H_2O were tentatively identified on the basis of their possible hydrogen bonding interactions with neighboring atoms using WingGX Calc-OH function. The O–H distances of these molecules were subsequently restraint at 0.83 Å and thermal parameters of $U_{iso(H)} = 1.2U_{eq(O)}$.

Table S1 Data collection parameters of **2**·$(OTf)_2$·$4H_2O$ and **3b**

	2·$(OTf)_2$·$4H_2O$ [a]	**3b**
Chemical formula	$C_{82}H_{80}Au_2F_{12}In_2O_{22}P_6S_4$ [a]	$C_{15}H_{14}NPS_2$
CCDC	1409234	1409233
FW, g mol^{-1}	2469.09	303.36
Crystal system	Monoclinic	Orthorhombic
Space group	$P2_1/n$	$P2_12_12_1$
a, Å	13.0061(6)	5.8353(4)
b, Å	26.0157(12)	10.1489(6)
c, Å	14.5344(6)	24.6603(15)
α (deg)	90	90
β (deg)	91.4340(10)	90
γ (deg)	90	90
Volume, $Å^3$	4916.4(4)	1460.43(16)
Z	2	4
ρ_{calcd}, Mg m^{-3}	1.850	1.380
μ, mm^{-1}	3.696	0.459
T (K)	223(2)	223(2)
No of reflections collected	28276	15109
No of independent reflections	8660 [R(int) = 0.0289]	3349 R(int) = 0.0273
No of parameters	564	172
GOF	1.217	1.122
R_1 and wR_2 [$I > 2\sigma(I)$]	R_1 = 0.0546 wR_2 = 0.1442	R_1 = 0.0403, wR_2 = 0.0973
R_1 and wR_2 (all data)	R_1 = 0.0587 wR_2 = 0.1497	R_1 = 0.0424, wR_2 = 0.0986
Large diff. peak and hole (e.$Å^{-3}$)	1.790 and -1.656	0.399 and -0.205

[a] The 8 H atoms from the non-coordinated H_2O molecules have not been included in the model.

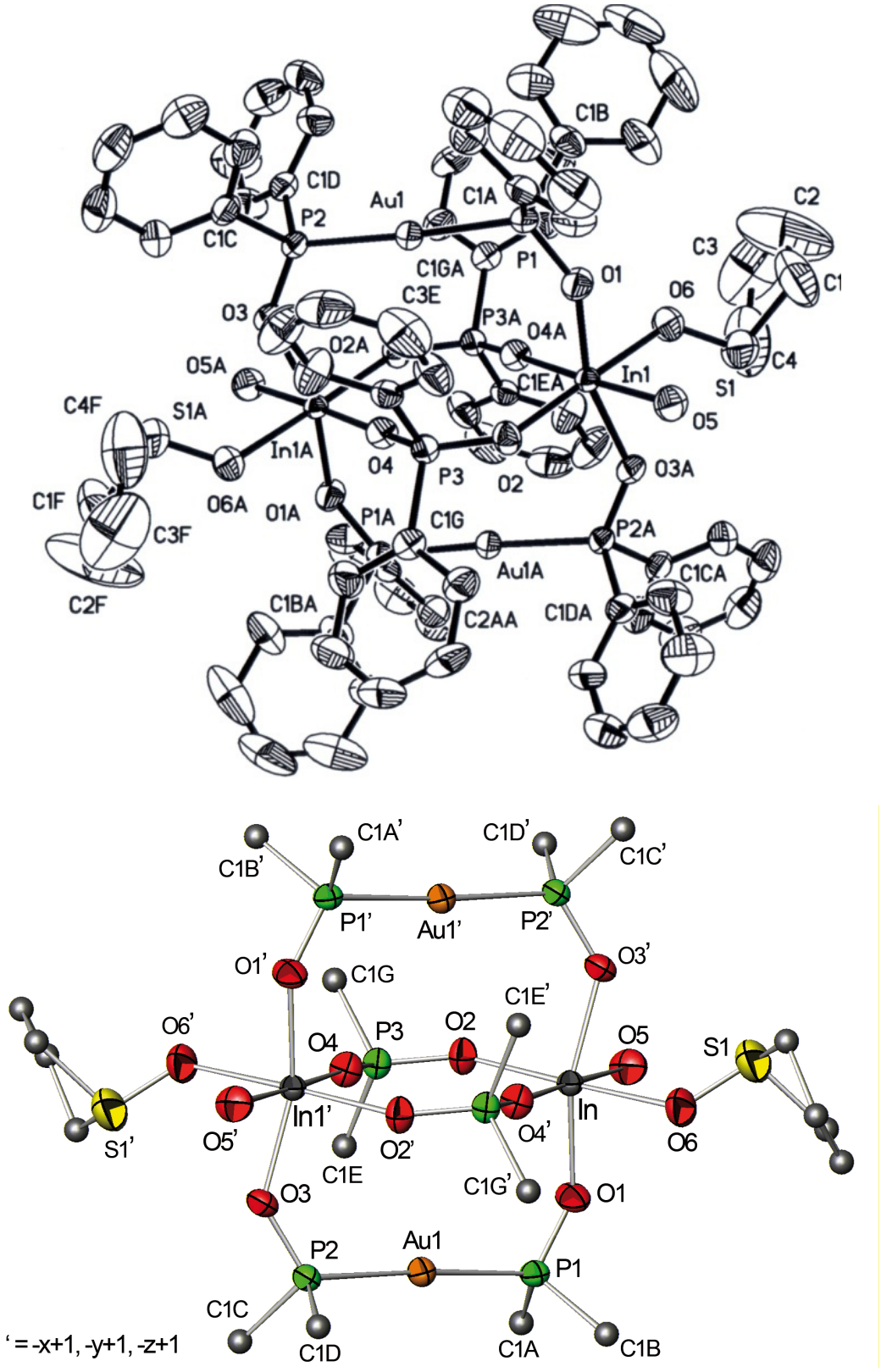

Figure S1. ORTEP diagrams with numbering scheme of the cation **2** in **2**·$(OTf)_2$·$4H_2O$ showing 50% probability ellipsoids. Top: all atoms, bottoms, only the ipso carbons of the phenyl groups are shown. Selected bond distances (Å): P(2)-O(3) 1.536(7) Å, P(1)-O(1) 1.527 (7) Å, P(3)-O(2) 1.513 (7) Å, P(3)-O(4) 1.506(6) Å.

X-ray Powder Diffraction

For the X-ray powder diffraction data, the powdered samples of **6'** and **7'** were analyzed using a Siemens D5005 X-ray diffractometer with Cu-Kα1 radiation (λ = 1.54056 Å), operated at 40 kV. The samples were placed on a plastic sample holder.

FESEM

FESEM was run on a JEOL 6701F Spectrometer, as an in-house analysis, at the National University of Singapore.

XPS

XPS studies were done as commercial samples by the laboratory at the Institute for Materials Research and Engineering, on a VG ESCA 220I-XL Imaging XPS, and processed on the Avantage software developed by Thermo Scientific. The spectra for **6'** and **7'** were calibrated using the C1s peaks as internal standards.

GC-MS

THT and the desired catalyst (2 mol %) under study were stirred under air for 3 days to 1 week in water or a mixture of water-THF (1:1). The product was extracted using CH_2Cl_2 and Et_2O, and the combined extracts were filtered through a short silica gel column to remove any metal particules before analysis. GC-MS for the control experiment using $In(OTf)_3$ for sulfoxidation was done on a Hewlett Packard HP6890 GC System coupled to a Hewlett Packard 5973 Mass Selective Detector at the Gas Chromatography lab at the National University of Singapore. For the catalytic studies involving **6'** and **7'**, an Agilent/Hewlett Packard 5973 GCMS in the Mass Spectrometry laboratory at the National University of Singapore. H_2O_2 was added as an oxidant in one study involving **7'**, and only in this case sulfoxides were observed. No catalytic activity was observed for **6'** under similar conditions.

Synthesis of {[Au(Ph$_2$PO)$_2$]$_2$In$_2$(Ph$_2$PO$_2$)$_2$(THTO)$_2$}(OTf)$_2$·4H$_2$O (**2**·(OTf)$_2$·4H$_2$O)

To a solution of [AuCl(THT)] (0.150 g, 0.468 mmol) in THF (50 mL), THT (0.08 mL, 0.907 mmol) was added, followed by Ag(OTf) (0.125 g, 0.481 mmol). The mixture was allowed to stir for 2 h and **1a** (0.275 g, 0.978 mmol) was added after removal of AgCl by filtration. In(OTf)$_3$ (0.270 g, 0.480 mmol) was added 2 h later and the solution was stirred overnight. The reaction mixture was filtered and allowed to stand in a sealed tube in the dark. Colourless crystals were obtained over 3 weeks. Washing with MeCN (3 x 5 mL) to remove the thiazol-2-amine hydrochloride gave a colourless powder of the product. Yield: 0.112 g, 19% (as **2**·(OTf)$_2$·4H$_2$O)**.** ^{19}F{^{1}H} NMR (D$_6$-acetone): δ = -2.5 ppm (s). ^{31}P{^{1}H} NMR (D$_6$-acetone): δ = 108.7 ppm (s, Ph$_2$*P*O$_2$), 27.1 (s, Ph$_2$*P*O). ^{1}H NMR (D$_6$-acetone): δ 6.31 (s, SC*H*$_2$), 6.60 (s, C*H*$_2$), 7.01-7.78 ppm (m, Ph). Peaks were too broad for good integration data, and it was not possible to discern coupling constants. The poor solubility of this complex also prevented recording of good quality ^{13}C{^{1}H} NMR spectra. ESI: *m/z* = 1660.7 ([Au$_2$(PPh$_2$O)$_4$In$_2$(PPh$_2$O$_2$)(PPh$_2$=O)]$^+$) (65%). Anal. Calcd. For **2**·(OTf)$_2$·4H$_2$O (%): C, 39.76; H, 3.58; S, 5.18. Found: C, 38.94; H, 3.66; S, 5.33. Despite several attempts, no better C analysis could be obtained.

THT oxidation control experiment using In(OTf)$_3$ in H$_2$O/THF for a week gave a *m/z* peak of 104 in the 11 min peak of the GC which corresponds to [THTO + H]$^+$, without the need to use any external oxidant. The long reaction time required to detect the product is possibly due to the ability of the THTO to coordinate to the metal centre, which may lead to an induction period where excess THTO has to be produced before it can be detected.

\3-Diphenylphosphanyl-thiazolidine-2-thione ligand **(3b)**

To a solution of thiazoline-2-thione (3.00 g, 25.4 mmol) in THF (50 mL), triethylamine was added in excess (5 mL) and liquid Ph$_2$PCl (4.58 mL, 26 mmol) was added dropwise. The

solution was stirred for 2 h, $Et_3N{\cdot}HCl$ was removed by filtration and the volatiles were removed under reduced pressure. The yellow oil obtained was redissolved in THF (100 mL) and layering the solution with hexane afforded colourless needles suitable for single crystal X-ray studies. Yield: 3.512 g, 46%. The ligand is highly air sensitive. Crystals of **3b** decomposed in a sealed Schlenk flask under nitrogen within a week. As a result of this, selected ^1H NMR data are given, whereas $^{13}C\{^1H\}$ data could not be obtained.

^1H NMR (CD_3CN): δ = 7.11-7.28 (m, Ph), 3.38 (t, NCH_2), 3.30 (t, SCH_2). $^{31}P\{^1H\}$ NMR (CD_3CN): δ = -39.8 ppm (s). ESI: *m/z* = 303.8 ($[M+H]^+$) (45%). Anal. Calcd. for **3b** (%): C 59.38, H 4.65, N 4.62; S, 21.14. Found: C, 59.60; H, 4.63; N 4.60; S, 20.83.

Synthesis of $[\{Au(Ph_2PO)_2\}_2In_2(Ph_2PO_2)_2(H_2O)_2(THTO)_2]_3(PO_4)_2$ (6)

The procedure used was similar to that for **2**, except that Ag_3PO_4 was used in lieu of Ag(OTf). Yield: 0.187 g, 43%. Anal. Calcd. for [**6**-2THTO-2H_2O], **6'**: C, 41.64; H, 2.94; S, 1.18; Found: C, 40.83 H, 2.94 S, 1.20. Despite several attempts, no better C analysis could be obtained.

The insolubility of the nanomaterial **6'** precluded other analyses. GC-MS monitoring of attempted sulfoxidation reactions revealed no formation of THTO after 3 days, either in water or in a H_2O-THF mixture.

Synthesis of $[\{Ag(Ph_2PO)_2\}_2In_2(Ph_2PO_2)_2(H_2O)_2(THTO)_2]_3(PO_4)_2$ (7)

The procedure used was similar to that for **2**, except that Ag_3PO_4 and THT were used to prepare $[Ag(THT)]_3(PO_4)$ in lieu of $[Au(THT)_2]OTf$. Yield: 0.193 g, 49%. Analytical data for [**7**-7.25THTO-6H_2O], **7'**: Anal. Calcd.: C, 46.22 H, 3.27 S, 1.78; Found: C, 48.59 H, 3.39 S, 1.78. Despite several attempts, no better C analysis could be obtained. The insolubility of the nanomaterial **7'** precluded other analyses. GC-MS monitoring showed the formation of the sulfoxidation product THTO (*m/z* 104.9) after 3 days when H_2O_2 was added as an oxidant.

Control experiments for the oxidation of THT were successfully performed using commercially available $In(OTf)_3$ in a H_2O-THF (1:1) mixture (**Figure S2**). In the absence of $In(OTf)_3$, no THTO was formed. Addition of THTO prepared *ex situ* by oxidation with H_2O_2, or addition of DMSO did not lead to **2**.

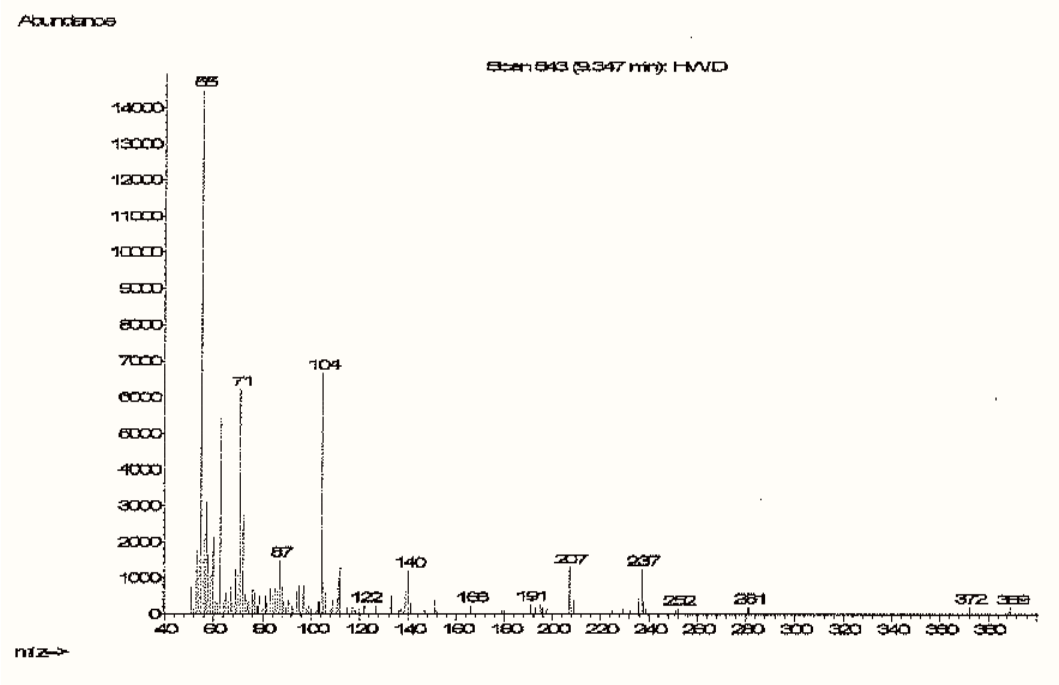

Figure S2. MS results for sulfoxidation with $In(OTf)_3$, showing the presence of THTO at a *m/z* value of 104, from GC-MS studies.

Preparation of the Au-In and Ag-In nanomaterials

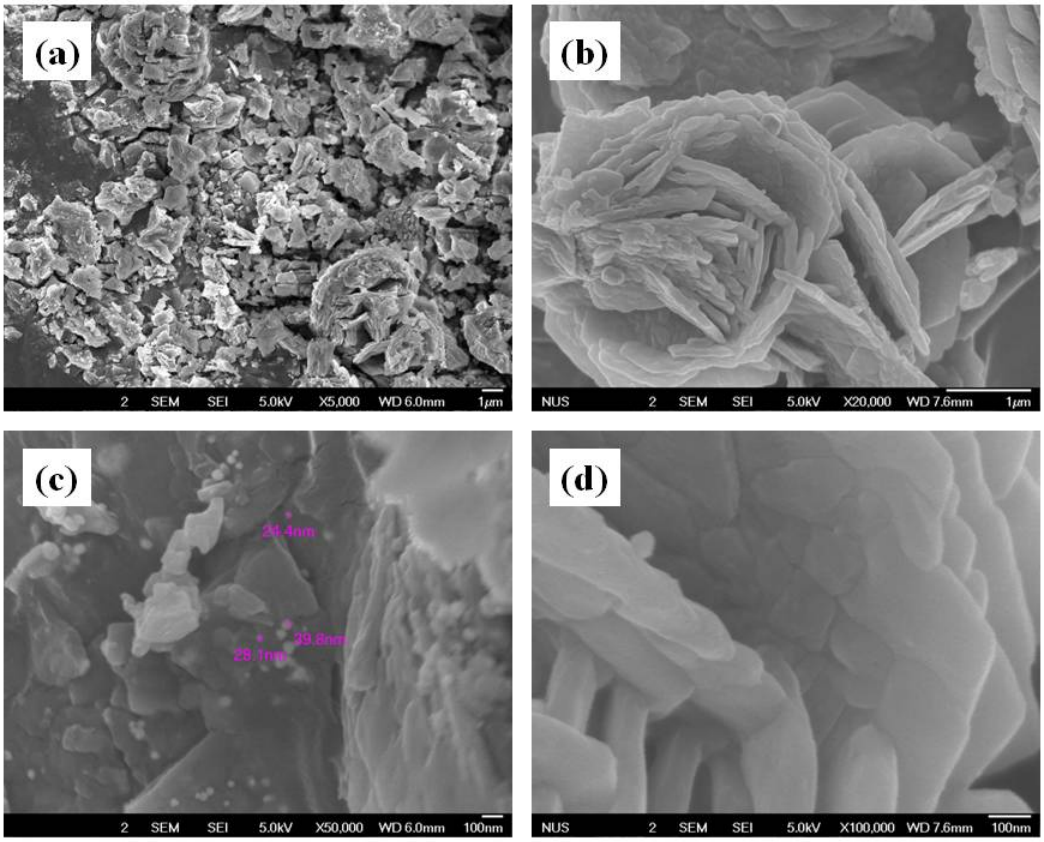

Figure S3. FESEM images of Au-In nanomaterial **6'**, at magnifications of (a) 5000, (b) 20000, (c) 50000 with measurements of individual particles, and (d) 100000 times.

The measurements in FESEM for both **6'** and **7'** showed plate-like structures of 86 nm thickness which are decorated with particles ranging from 25-40 nm. (Figures S3 and S4)

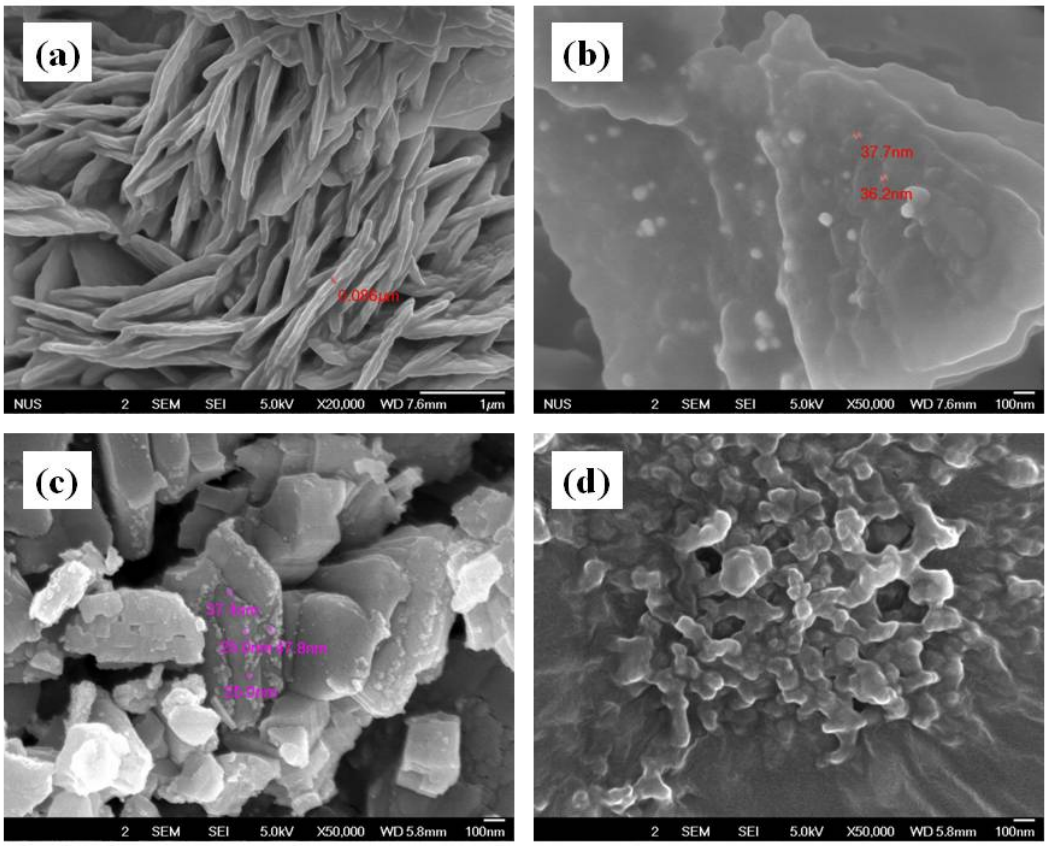

Figure S4. FESEM Images of Ag-In nanomaterials **9'**, at magnifications of (a) 20000 with measurements on plate thickness, 50000 with measurements of individual particles, (c) 50000 showing cuboids and (d) 50000 times showing bone-like structures.

Figure S5. Image of Au-In and Ag-In nanomaterials **6'**and **7'**.

The use of Ag in place of Au led to a metallic olive-green Ag-In solid, **7'**, compared to the reddish brown colour of Au-In **6'**. (Figure S5)

X-ray Photoelectron Spectroscopy (XPS) studies on **6'** showed the presence of Au, In and PO_4 (Figure S6); and on **7'** likewise the presence of Ag, In and PO_4 (Figure S7), further confirming the heterobimetallic nature of the materials.[6]

The binding energy in the XPS is shifted with respect to known standard values, but it is noteworthy that XPS, though a valuable tool for determining the oxidation state of a metal, should be used with caution for nanoparticles in a non-conductive polymeric environment because, in some cases, high binding energy values can be due to charging of the nanoparticles. As a result, a higher oxidation state is demonstrated than that actually present in a real sample. Normally, comparison with the XRD data allows one to clarify this issue.[7]

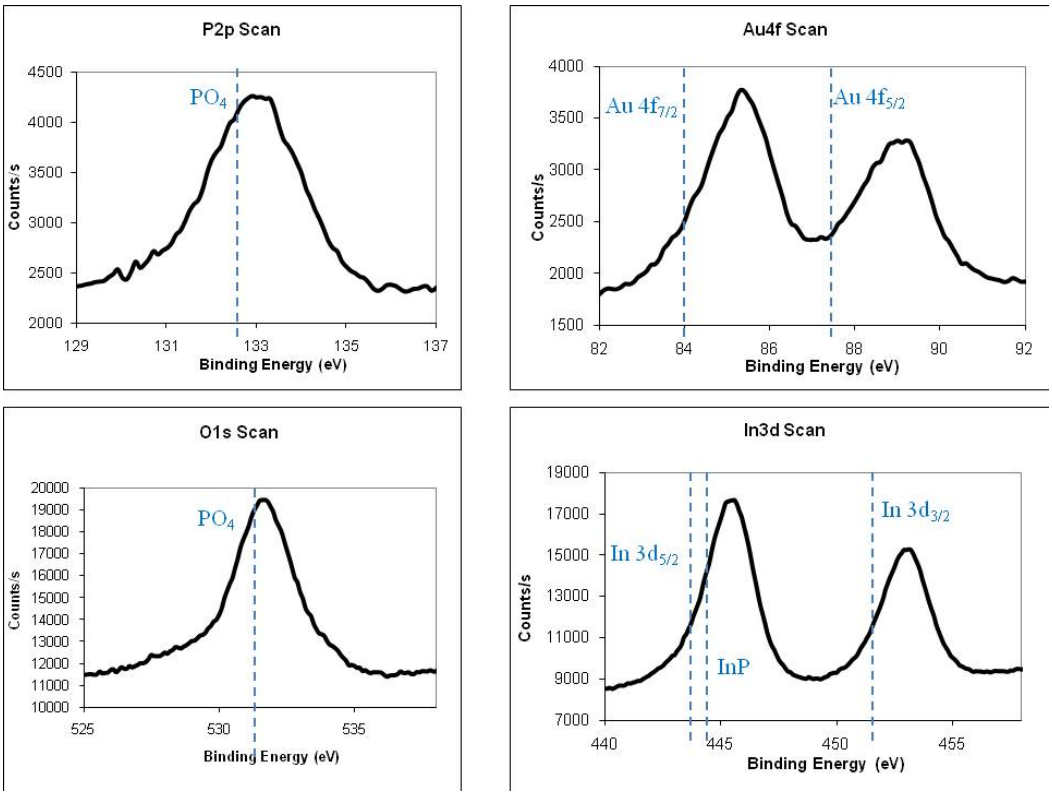

Figure S6. XPS spectra for **6'**.

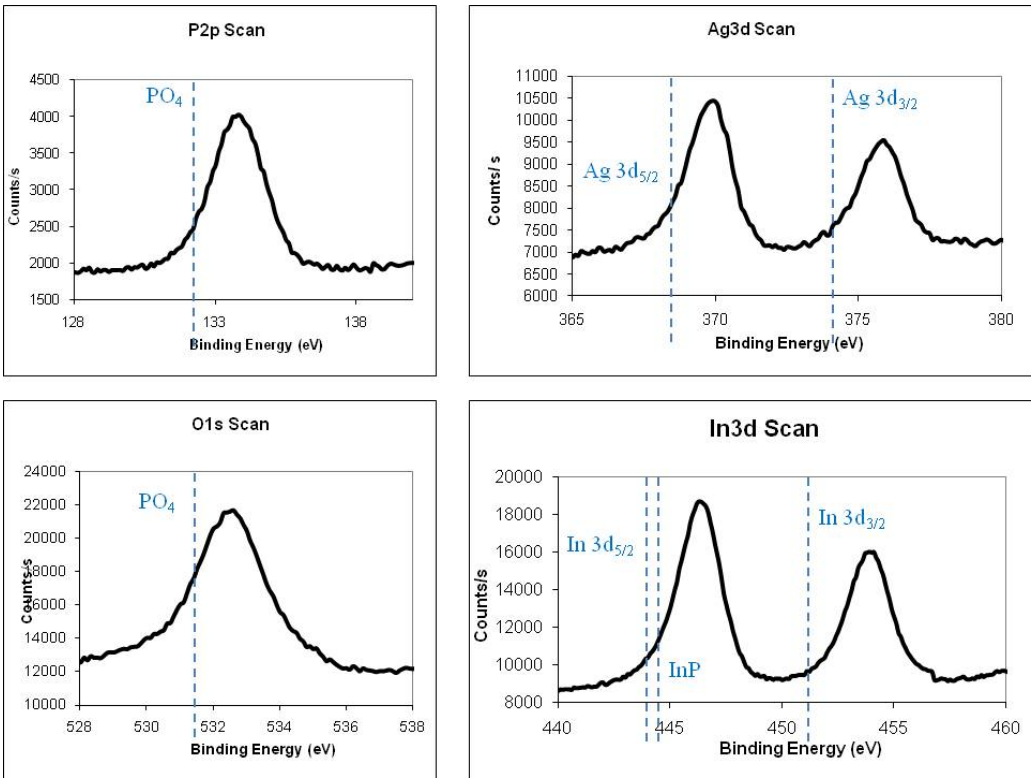

Figure S7. XPS spectra for **7'**.

Nanomaterials **6'** and **7'** were tested as heterogeneous catalysts for the sulfoxidation of THT, but GC-MS studies showed no formation of THTO under aerobic conditions. This further supports the fact that $In(OTf)_3$ is the catalyst for sulfoxidation during formation of complex **2.** In one instance, H_2O_2 was added as the oxidant for sulfoxidation with **7'**, and some THTO was detected in this case. (Figure S8). Thus, **7'** possess sulfoxidation potential, but only in the presence of H_2O_2 as oxidant. No catalytic activity was observed with **6'** after 3 days of reaction, either in H_2O-THF or in the presence of added H_2O_2.

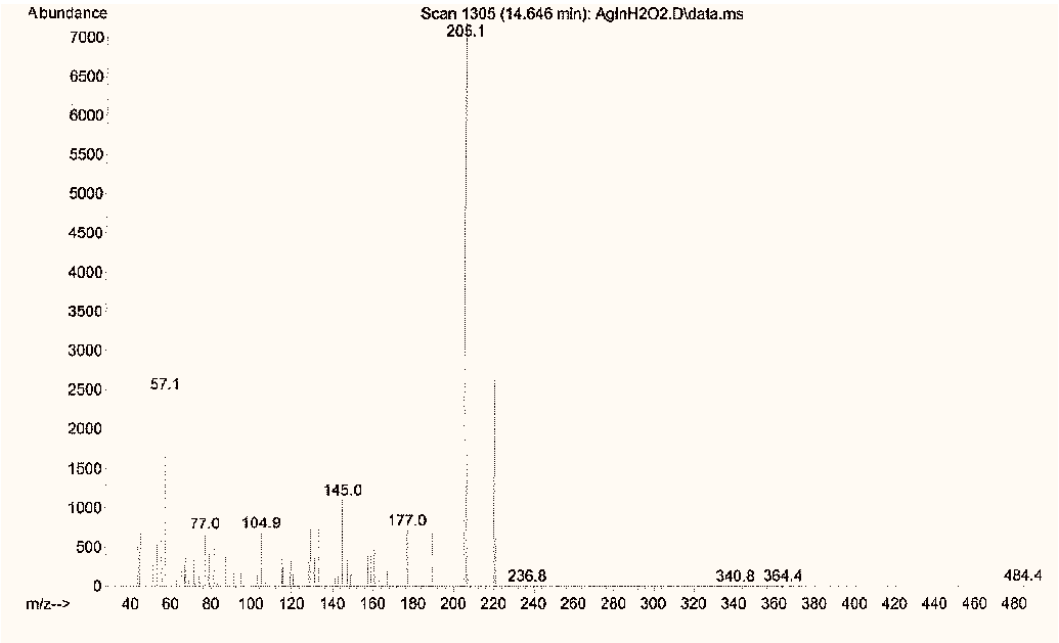

Figure S8. Mass spectrometry results for the sulfoxidation reaction with **7'** and H_2O_2, showing the presence of THTO at a *m/z* value of 104, from GC-MS studies.

FESEM studies

As charging was observed during the FESEM studies, the XPS results were not overly emphasized as being significant. Powder X-ray diffraction (XRD) of **6'** and **7'** were largely amorphous (Figures S9 and S10), and did not reveal any useful information. This is

unsurprising given the expected collapse of the crystalline structure by loss of THTO either in the baking process or while grinding on a jade mortar and pestle.

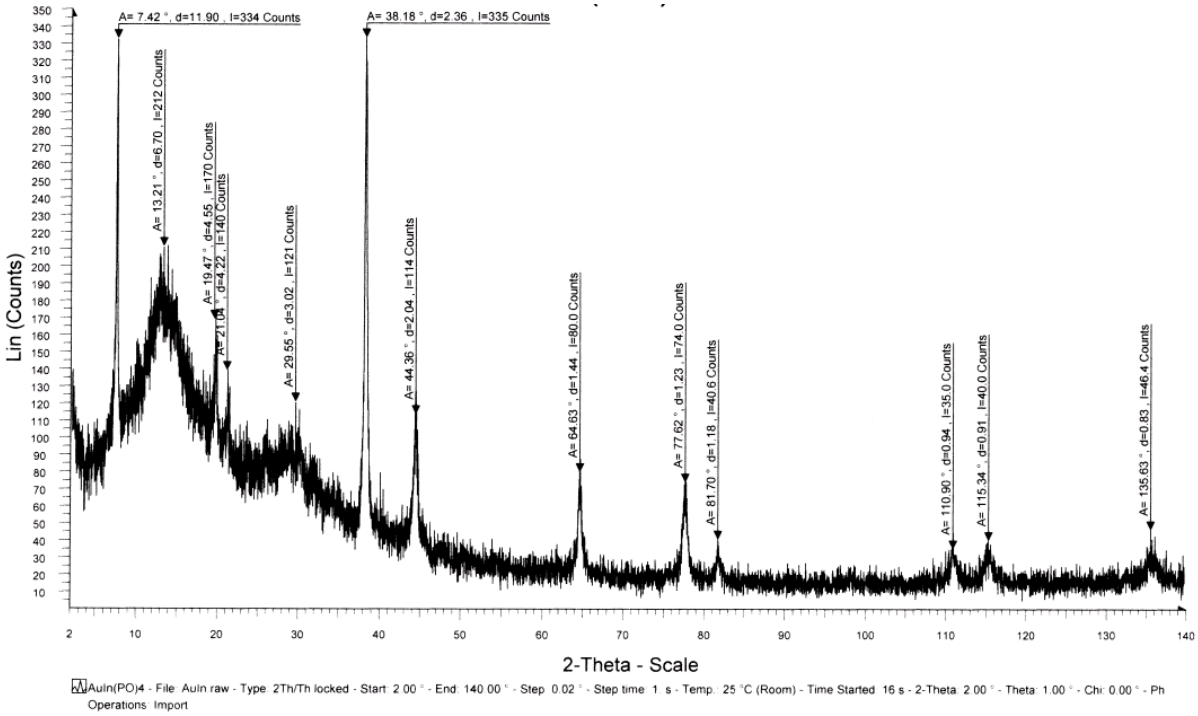

Figure S9. Powder XRD data of **6'**.

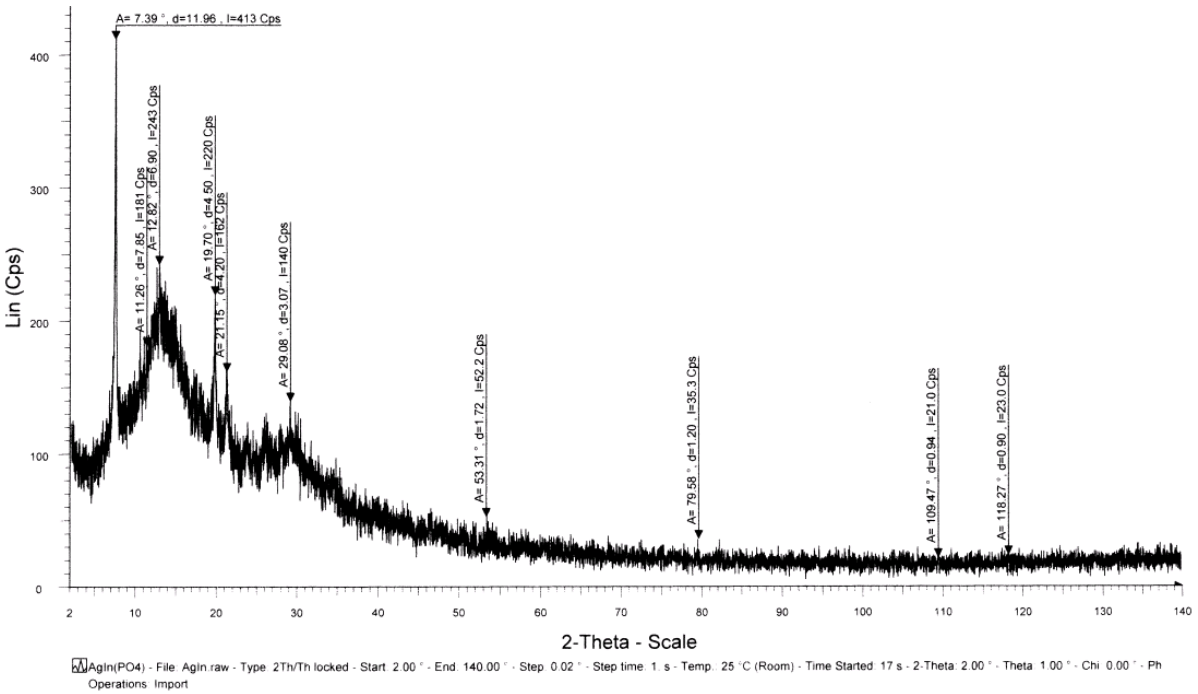

Figure S10. Powder XRD data of **7'**.

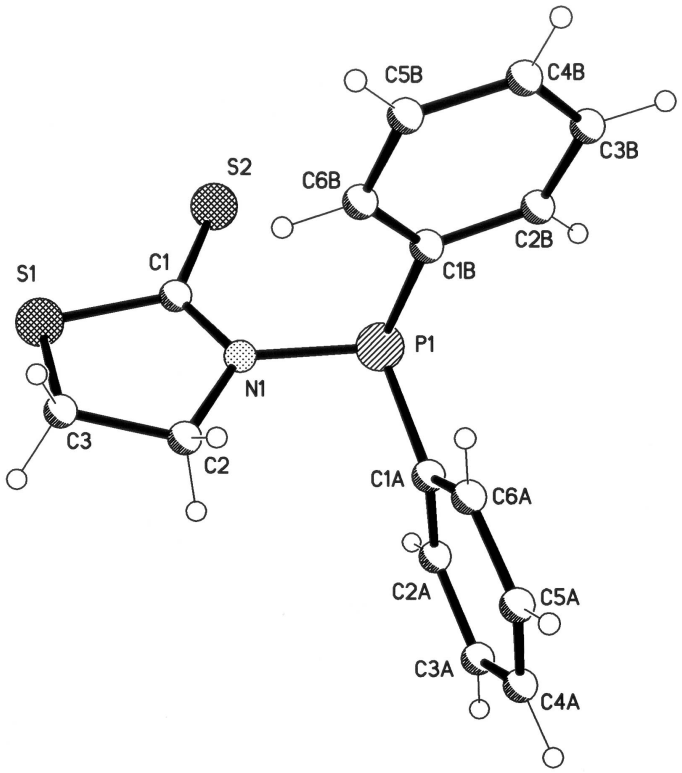

Figure S11. Ball and stick view of **3b**. Displacement parameters include 50% of the electron density. Selected bond distances (Å) and angles (º): P(1)-N(1) 1.760(2), C(1)-S(1) 1.739 (2), C(1)-N(1) 1.338 (3), C(1)-S(2) 1.664(2), S(1)-C(3) 1.793(3), C(3)-C(2) 1.507(3), C(2)-N(1) 1.475(3); C(1)-N(1)-C-(2) 115.8 (2), C(1)-N(1)-P(1) 118.2 (2), C(2)-N(1)-P(1) 125.6 (2).

[1] R. Uson, A. Laguna and M. Laguna, *Inorg. Synth.,* 1989, **26**, 85.

[2] (a) H. L. Milton, M. V. Wheatley, A. M. Z. Slawin and J. D. Woollins, *Inorg. Chim. Acta* 2005, **358**, 1393; (b) O. Kühl, B. Walfort and T. Rüffer, *Crystal Growth & Design,* 2006, **6**, 366.

[3] SMART (Version 5.631) and SAINT (Version 6.63) Software Reference Manuals, Bruker AXS GmbH, Karlsruhe, Germany, 2000.

[4] G. M. Sheldrick, SADABS: a Software for Empirical Absorption Correction; University of Göttingen: Göttingen, Germany, 2001.

[5] SHELXTL Reference Manual, Version 6.10; Bruker AXS GmbH, Karlsruhe, Germany, 2000.

[6] (a) H. Çetin, E. Ayyildiz and A.Turut, *J. Vac. Sci. Technol*., B, 2005, **23**, 2436; (b) H. Çetin and E. Ayyildiz, *Physica B*, 2007, **394**, 93; (c) H.-G. Boyen, A. Ethirajan, G. Kästle, F. Weigl, P. Ziemann, G. Schmid, M. G. Garnier, M. Büttner and P. Oelhafen, *Phys. Rev. Lett.*, 2005, **94,** 016804; (d) J. R. Waldrop, S.P. Kowalczyk and R. W. Grant, *Appl. Phy Lett.*, 1983, 42, 454; (e) A. Pakes, P. Skeldon, G. E. Thompson, R. J. Hussey, S. Moisa, G. I. Sproule, D. Landheer and M. J. Graham, *Surf. Interface Anal.*, 2002, **34**, 481.

[7] L. M. Bronstein, G. D. Matveeva and E. M. Sulman, in: D. Astruc (Ed.), *Nanoparticles and Catalysis*, Wiley-VCH, Weinheim, 2008.